

Photoinduced Removal of the Franck–Condon Blockade in Single-Electron Inelastic Charge Transmission

Volkhard May* and Oliver Kühn†

Institut für Physik, Humboldt-Universität zu Berlin, Newtonstrasse 15, D-12489 Berlin, Germany, and Institut für Chemie und Biochemie, Freie Universität Berlin, Takustrasse 3, D-14195 Berlin, Germany

Received December 3, 2007; Revised Manuscript Received February 5, 2008

ABSTRACT

A new mechanism of charge transmission through a metal–molecule–metal junction is suggested that is based on optical driving of electronic transitions in the neutral and singly charged molecular state. The effects of strong electron vibrational coupling, intramolecular vibrational energy redistribution, and molecular de-excitation caused by electron–hole pair formation in the leads are taken into account. It is shown that current suppression due to the Franck–Condon blockade can be overcome by opening new transmission channels via photoexcitation.

Understanding the details of charge transport through nanostructures is of tremendous importance for technological realization of molecular electronic devices.^{1,2} Current flow through single or composite metal or semiconducting nanoparticles has been intensively investigated (see, e.g., ref 3). While in these structures the electronic spectrum dominates the transport with only marginal contributions from lattice motions (phonons), nuclear rearrangement (NR) during charge transmission may strongly influence the transport through metal–molecule–metal junctions.⁴ Here, the electronic levels are “dressed” by vibrational states and the resulting spectrum may depend considerably on the actual electronic state. In terms of the associated electron–vibrational dynamics, this implies that a pronounced nonequilibrium vibrational distribution within the electronic states may be established in the stationary regime of current flow. This triggers novel effects such as the Franck–Condon blockade, i.e., the suppression of current flow at low bias voltages.⁵ The shape of the distribution which is established and thus the current–voltage (*IV*) characteristics not only depends on NR but also on the time scale of intramolecular vibrational energy redistribution (IVR).⁶

The interaction with external electromagnetic fields could provide a means to control the current flow in metal–molecule–metal junctions, a topic that is moving into the realm of experimental realization.⁷ Theoretical studies based

on a tight-binding model including the coupling to a continuous-wave radiation field predicted effects such as coherent current suppression and nonadiabatic electron pumping.⁸ Laser pulses accounted for in such model Hamiltonians have not only proven to yield an efficient and robust current switching but at the same time operate on a time scale of a few hundred femtoseconds.^{9,10} A coupling to a radiation field in the optical range including photon emission via recombination has been considered in refs 11, 12 within a HOMO–LUMO scheme and in ref 13 using energies and matrix elements from a many-body calculation. On the other hand, optical excitation of charge transfer states may lead to an additional driving force for current flow.¹²

In this contribution we discuss the *IV* characteristics of single-molecule charge transfer subject to the combined influence of continuous-wave photoexcitation of electronic transitions and strong NR of a molecular reaction coordinate whose nuclear wave packet dynamics is damped due to IVR. Using a master equation approach developed previously,^{6,14} we demonstrate that the Franck–Condon blockade can be overcome due to the opening of new transmission channels that are robust with respect to molecular de-excitation caused by electron–hole pair formation. The paper is organized as follows. In the next section, we will discuss the model for incorporating nuclear rearrangement and introduce the spectral density of vibrational wave function overlap as the central quantity for characterization of electron–vibrational coupling. Subsequently, the rate equations are introduced and the working equation for the calculation of the current is

* Corresponding author. E-mail: may@physik.hu-berlin.de.

† New address: Institut für Physik, Universität Rostock, Universitätsplatz 3, D-18051 Rostock, Germany.

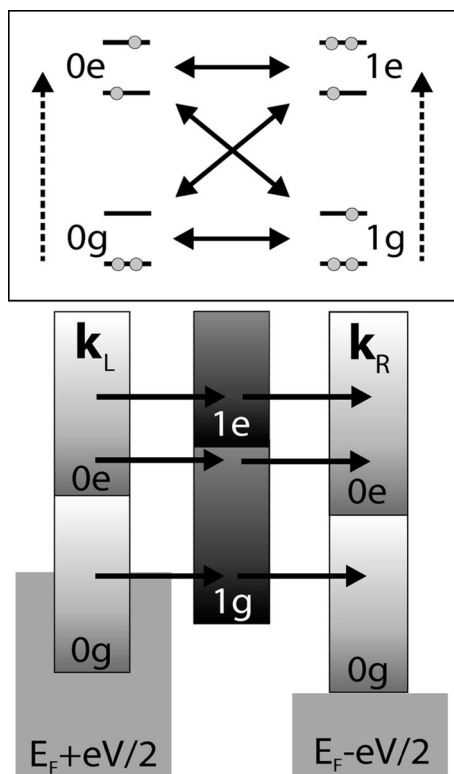


Figure 1. Schematic view of possible charge transfer (solid arrows) and photoinduced (dashed arrows) transitions. Upper panel: ground- and excited-state electronic configurations in a HOMO–LUMO scheme referring to the neutral and singly charged molecule. Lower panel: electron-vibrational state manifolds for the neutral ($N = 0$) and charged (dark grey boxes, $N = 1$) states in the electronic ground (N_g) and excited (N_e) configurations. Lead electron energies are shown before (k_L) and after (k_R) charge transfer. The model assumes a symmetrically applied voltage V , and the respective positions of the lead’s chemical potentials are indicated. Note that not all channels of the upper panel are open in the lower configuration.

given. This is followed by a presentation of numerical results and a summary.

Nuclear Rearrangement. We consider the neutral ($N = 0$) and the singly charged ($N = 1$) state of a molecule attached to a left ($X = L$) and a right ($X = R$) lead. The cationic state $N = -1$ is assumed to be energetically well separated and thus negligible, see also ref 13. Both charging states are further characterized by two electronic configurations, that is, the ground state with energy $\hbar\epsilon_{N_g}$ and the first excited state with energy $\hbar\epsilon_{N_e}$ (see Figure 1). Charge transfer between the neutral and singly charged states is due to the couplings $V_X(0a, 1b; \Omega)$ ($a, b = g, e$) as indicated by solid arrows in Figure 1. Note that we combine the electronic energy of the neutral molecule with the continuum of lead electron energies for a given k -vector into the energy $\hbar\epsilon_{ka}$.

Using this model current suppression has been demonstrated in ref 5 for applied voltages smaller than $E_{10} + \lambda_{10}$. Here, $E_{10} = \hbar(\epsilon_{1g} - \epsilon_{0g}) - \mu_0$, with μ_0 being the equilibrium chemical potential of the leads and λ_{10} denotes the nuclear reorganization energy upon charging. This Franck–Condon blockade of current flow is due to the small overlap $\langle\chi_{0g\mu}|\chi_{1gv}\rangle$ of those vibrational wave functions of the neutral as well as

the charged molecule whose energy is smaller than λ_{10} ($|\chi_{Na\mu}\rangle$ are the vibrational states for charging state N , electronic state a , and vibrational state μ). Unless IVR is rapid, the Franck–Condon blockade is connected to a pronounced nonequilibrium distribution across the vibrational levels.⁶

NR is not only a consequence of charging but nonequilibrium vibrational distributions are independently obtained by optical excitation from the electronic ground to the first excited state, as shown by the dashed arrows in Figure 1. This opens new photoinduced charge transfer channels where a particularly interesting situation occurs if the combined energy $\hbar\epsilon_{ke}$ belongs to a lead electron deep in the Fermi-sea such that $\hbar\epsilon_{ke} \approx \epsilon_{1g}$. In this case, optical excitation moves the neutral molecule into its excited state and charging of the molecule in its electronic ground state becomes possible, i.e., $0e \rightarrow 1g$. Because a rather large set of the $\hbar\epsilon_{ke}$ may be involved, a multitude of vibrational levels of the electronic ground state of the charged molecule will be populated. In the stationary case, this nonequilibrium population acts back via discharge on the stationary vibrational level populations of the neutral molecule in its electronic ground state via $1g \rightarrow 0g$. As will be shown below, the nonequilibrium population that is established by this mechanism in the neutral ground state allows overcoming of the Franck–Condon blockade.

The shifted oscillator model provides a reasonable description for electron-vibrational coupling in molecules.¹⁵ Here the electronic energies $\hbar\epsilon_{Na}$ are “dressed” by the following potential energy surfaces (PES) for nuclear motion along some reaction coordinate Q having frequency ω_{vib} :

$$U_{Na}(Q) = \hbar\omega_{\text{vib}}(Q - Q_{Na})^2/4 \quad (1)$$

Notice that for simplicity we assume the vibrational frequency to be state independent. The coupling to a charge transfer or optical transition is quantified by the PES shift Q_{Na} . The reorganization energies are

$$\lambda_{Ma,Nb} = \hbar\omega_{\text{vib}}(Q_{Ma} - Q_{Nb})^2/4 \quad (2)$$

Their values can be used to identify reaction coordinates out of the many molecular nuclear degrees of freedom. The mutual shifts of the PES also define the related Franck–Condon factors. Within the rate description given below, the Franck–Condon physics is conveniently expressed via the spectral density of vibrational wave function overlap (SDVO)

$$S_{Ma,Nb}(\omega, \bar{\omega}) = \sum_{\mu,\nu} \delta(\omega - \omega_{Ma\mu}) \delta(\bar{\omega} - \omega_{Nb\nu}) |\langle\chi_{Ma\mu}|\chi_{Nb\nu}\rangle|^2 \quad (3)$$

where $\omega_{Ma\mu} = \mu\omega_{\text{vib}}$ for the present model. This function is shown in Figure 2 for the cases considered below. It nicely demonstrates that effective transitions are restricted to a narrow range in the $(\omega, \bar{\omega})$ plane. Of course, the actual shape of the SDVO not only depends on the PES shifts but would also reflect differences in vibrational frequencies of the electronic states. In passing, we note that the definition of the SDVO is straightforwardly extended to the multimode case. It is to be expected that, with increasing number of modes having different frequencies, the sharp features in Figure 2 are smeared out.

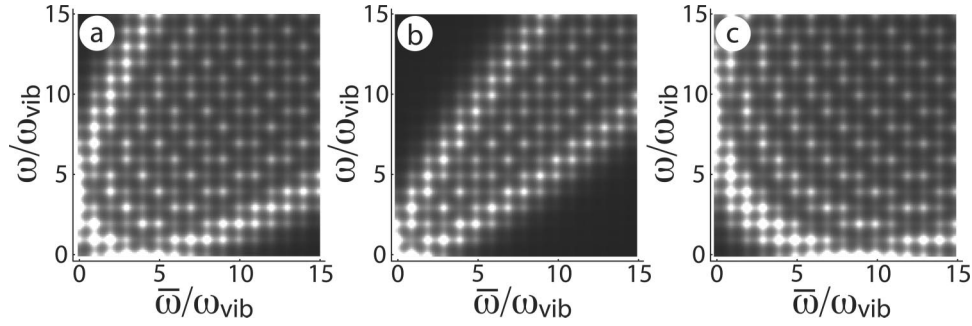


Figure 2. Contour plot of the SDVO, eq 3, vs ω and $\bar{\omega}$ assuming a Lorentzian type broadening by $0.3\omega_{\text{vib}}$. For the minima of the PES chosen as $Q_{0g} = 0$, $Q_{0e} = 4$, $Q_{1g} = 6$, and $Q_{1e} = 2$, the SDVOs correspond to optical excitation (a), charging from the electronic excited into the ground state (b), and discharge between the ground states (c).

Rate Equations and Current Formula. The theoretical analysis of the radiation field driven charge transmission through a single molecule has to account for NR of the reaction coordinate as well as IVR due to their coupling to the remaining bath modes. The latter are assumed to have negligible reorganization energy upon charging and optical transition. In the terminology of solid-state theory, strong electron–phonon coupling has to be combined with a proper description of nonequilibrium phonon distributions. At present, both effects cannot be tackled either by applying time-dependent DFT or nonequilibrium Green’s functions.² An appropriate tool, however, are generalized rate equations governing vibrational distribution functions. Respective rate expressions can be deduced from the general master equation kernel:^{6,14}

$$K_{Ma \rightarrow Nb}(t, \bar{t}) = \text{tr}\{\hat{\Pi}_{Nb} T(t, \bar{t}) \hat{W}_{Ma}\} \quad (4)$$

where the trace is defined in the total space of lead–molecule states, \hat{W}_{Ma} is the initial statistical operator of the whole system (at given applied voltage) referring to a particular electron–vibrational state, and $\hat{\Pi}_{Nb}$ projects on the final electron–vibrational state. The transfer superoperator $T(t, \bar{t})$ contains all effects of interest and will be calculated employing perturbation theory.

In the stationary (nonequilibrium) regime, the generalized master equation for the electron–vibrational state populations, $P_{Ma}^{(\text{stat})}(\omega)$, can be written in the following form:

$$P_{Ma}^{(\text{stat})}(\omega) \tau_{Ma}^{-1}(\omega) = \sum_{Nb} \int d\bar{\omega} P_{Nb}^{(\text{stat})}(\bar{\omega}) k_{Nb \rightarrow Ma}(\bar{\omega}, \omega) \quad (5)$$

with the inverse lifetime being $\tau_{Ma}^{-1}(\omega) = \sum_{Nb} \int d\bar{\omega} k_{Ma \rightarrow Nb}(\omega, \bar{\omega})$. Notice that this general form accommodates not only the situation of a single reaction coordinate but also the case of many-coupled nuclear coordinates forming a continuous distribution in ω . The rates, $k_{Ma \rightarrow Nb}$ follow from the zero-frequency Fourier-transformed general master equation kernels and account for transitions among different electronic levels with vibrational continuum ω and $\bar{\omega}$, respectively, as well as for vibrational relaxation within an electronic state (for details, see ref 14).

Within second-order perturbation theory, all interstate rates can be expressed in terms of the SDVO defined in eq 3. Assuming weak molecule–lead coupling together with a broadband approximation, one can introduce the frequency-independent level broadening $\Gamma = 2\pi \bar{N}|\bar{V}|^2$ with mean

DOS of the leads, \bar{N} , and the mean transfer coupling \bar{V} . This gives the charging rate as:^{5,6,14}

$$k_{0a \rightarrow 1b}^{(\text{mol-lead})}(\omega, \bar{\omega}) = 4\Gamma S_{0a,1b}(\omega, \bar{\omega}) \sum_{X=L,R} f_F(\hbar(\epsilon_{1b,0a} + \bar{\omega} - \omega) - \mu_X) \quad (6)$$

Here, f_F denotes the Fermi function and μ_X is the chemical potential of lead X under applied voltage. The rate $k_{1b \rightarrow 0a}^{(\text{mol-lead})}(\bar{\omega}, \omega)$ of discharge is obtained by replacing f_F by $1 - f_F$ in the charging rate. The rate for optical excitation with a monochromatic field takes the form

$$k_{\text{Neg}}^{(\text{opt})}(\omega, \bar{\omega}) = 2\pi E_R^2 S_{\text{Ne,Ng}}(\omega, \bar{\omega}) L(\omega_0 - \epsilon_{\text{Ne,Ng}} - \omega + \bar{\omega}, \gamma) \quad (7)$$

where $E_R = \mathbf{d}\mathbf{E}$ is the Rabi energy (transition dipole moment \mathbf{d} times field strength \mathbf{E}). For simplicity, we assumed that the Rabi energy does not depend on the charging state. The line shape of optical transition is given by the Lorentzian $L(\omega, \gamma) = \gamma/\pi(\omega^2 + \gamma^2)$. The photon energy $\hbar\omega_0$ is assumed to be resonant to a vertical Frank–Condon transition. It is straightforward to extend the present description to the case of different excitation energies and transition dipole moments, e.g., by applying two fields. Finally, radiative and nonradiative decay is considered via

$$k_{\text{Neg}}^{(\text{dec})}(\omega, \bar{\omega}) = r_{\text{dec}} S_{\text{Ne,Ng}}(\omega, \bar{\omega}) \quad (8)$$

Intrastate transitions due to IVR will be described by a bilinear coupling model for the interaction between the reaction coordinate and the bath modes. In this case, the rate of IVR is determined by the reservoir spectral density taken at ω_{vib} , $J = J(\omega_{\text{vib}})$ (assumed to be state-independent).^{6,14,15}

The total stationary current can be obtained from the rate expressions describing the molecule–lead coupling as well as from the level populations, $P_{Ma}^{(\text{stat})}(\omega)$, as

$$I_{\text{tot}} = \sum_{a,b=g,e} (I_{0a \rightarrow 1b} + I_{1a \rightarrow 0b}) \quad (9)$$

In the present form, it allows for the investigation of the separate contributions due to the partial currents $I_{0a \rightarrow 1b}$ and $I_{1a \rightarrow 0b}$ describing charging and discharge of the molecule, respectively (cf. Figure 1).

Optical Field Control of Current Flow. Photoinduced charge transfer will be studied for the case of a single reaction coordinate with frequency $\omega_{\text{vib}} = 10\Gamma$, weakly coupled to a bath at low temperature ($k_B T = 0.5\hbar\Gamma$) and for $E_{10} = 40\hbar\Gamma$.

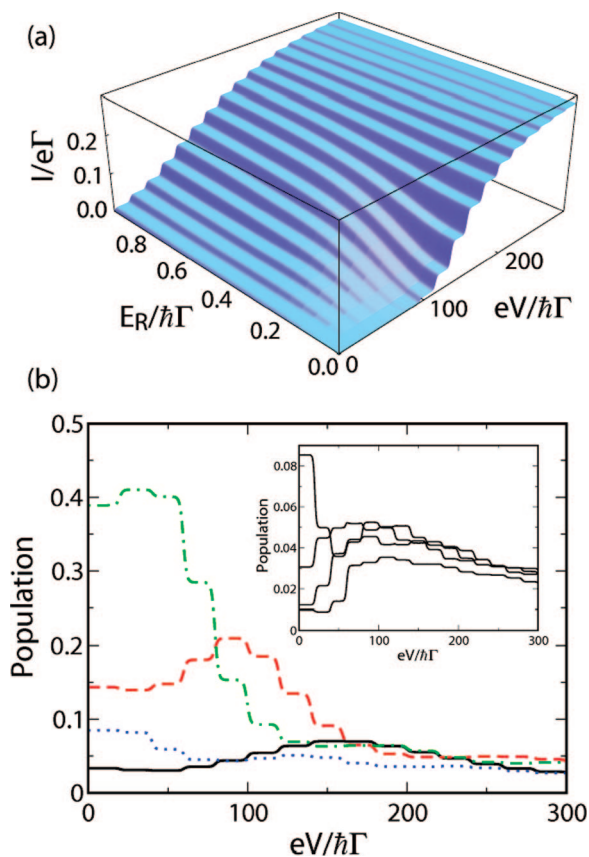


Figure 3. (a) Total current I_{tot} , eq 9, vs applied voltage and external field strength ($r_{\text{dec}} = J = 0$). (b) Stationary vibrational populations in the electronic ground state of the neutral molecule, $P_{0\mu}$, for $E_R = \hbar\Gamma$. (solid line: $\mu = 0$, dashed line: $\mu = 1$, dashed–dotted line: $\mu = 2$, dotted line: $\mu = 3$; Inset: $\mu = 4 \dots 7$ from bottom at $V = 0$).

The PES shifts are given in the caption of Figure 2 and correspond to the following reorganization energies: $\lambda_{0g,1g} = 90\Gamma$, $\lambda_{0g,0e} = \lambda_{1g,1e} = 40\Gamma$, and $\lambda_{0e,1g} = \lambda_{0e,1e} = 10\Gamma$.

Figure 3a shows the IV characteristics as a function of the Rabi energy; the used value for E_R corresponds to field strengths of $\sim 10^6$ V/cm (intensity range of some GW/cm²) for $\hbar\Gamma \sim 1$ meV and if the transition dipole moment lies in the range of a few Debye. For this special choice of Γ , the vibrational frequency would be equal to 10 meV, i.e., in a range as observed in previous low-temperature experiments (see, e.g., ref 4). In the absence of optical excitation, the current is exponentially blocked up to $|e|V = 100\hbar\Gamma$, which is a consequence of the small Franck–Condon overlap entering the rates via the SDVO, cf. Figure 2b. The current increases to its asymptotic value if $|e|V/2$ approaches $E_{10} + \lambda_{1g,0g} = 130\hbar\Gamma$. Notice that the steplike structure would give rise to a sequence of equidistant peaks in the conductivity similar to what has been observed previously.⁴

The current blocking is removed if ground–excited state transitions are driven by an external field. A detailed analysis shows that, for the given parameters, the transfer channel from the optically excited neutral molecule corresponding to \mathbf{k} -states deep in the Fermi-sea via the ground state of the charged molecule and back to the ground state of the neutral molecule is responsible for overcoming the Franck–Condon

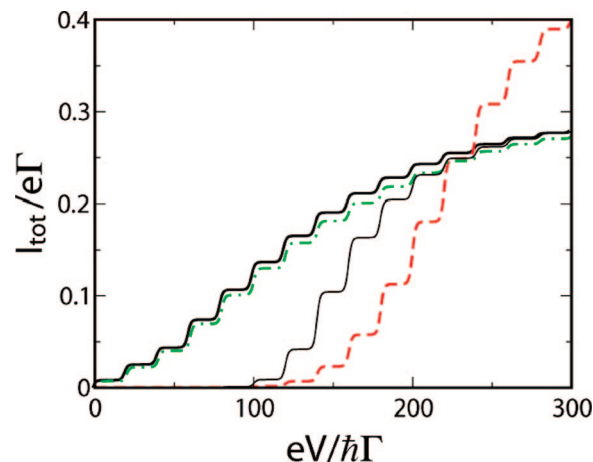


Figure 4. Total currents, eq 9, for $E_R = \hbar\Gamma$ and $J = 0$, $r_{\text{dec}} = 0$, full line; $J = \Gamma$, $r_{\text{dec}} = 0$, dashed line; $J = 0$, $r_{\text{dec}} = 100\Gamma$, dash–dotted line. The case of no optical excitation ($E_R = J = r_{\text{dec}} = 0$) is shown as a thin solid line.

blockade (cf. Figure 1). The channel involving optical excitation of the charged molecule is of minor importance. Analyzing the total current in terms of the partial currents according to eq 9, we find that I_{tot} is dominated by $I_{0g \rightarrow 1g}$ over the whole interval in Figure 3 except the low-voltage high-Rabi energy range where the contributions from $I_{0e \rightarrow 1e}$ and $I_{0e \rightarrow 1g}$ become comparable.

The role of the reaction coordinate can be discussed with the help of the SDVO introduced in eq 3. For the given temperature, the neutral molecule is initially in its vibrational ground state. Because of the form of $S_{Ne,Ng}(\omega, \bar{\omega})$ (cf. Figure 2a), optical excitation populates vibrational levels in the excited-state around $\nu = 4$. The SDVO for charging from this state, $S_{0e1g}(\omega, \bar{\omega})$ (cf. Figure 2b), favors transitions from $\omega = 4\omega_{\text{vib}}$ to $\bar{\omega} = 2\omega_{\text{vib}}$. The rate for subsequent discharge is proportional to $S_{1g,0g}(\omega, \bar{\omega})$, which, according to Figure 2c, is large for transitions from $\omega = 2\omega_{\text{vib}}$ to $\bar{\omega} = 2\omega_{\text{vib}} \dots 4\omega_{\text{vib}}$. Although the detailed form of the vibrational distributions depends on all possible channels according to eq 5, this estimate already indicates that, in the regime of stationary current flow, the reaction coordinate is kept in a nonequilibrium state. This can be seen from Figure 3b for the case of the largest Rabi energy of panel a. Notice further that the distribution tends to become similar among the lowest states for large bias voltages where all possible channels contribute, as there are no restrictions concerning energy conservation. This is also the limit where optical excitation is less important.

So far we have considered neither IVR nor radiative or nonradiative decay, and the question arises whether the suggested current switching is robust with respect to these processes. In Figure 4, we show the IV characteristics for different values of the IVR coupling strength, J , the decay rate, r_{dec} , and for a large Rabi energy. While the optical switching of the current survives IVR strength up to $J = 0.1\Gamma \dots 0.3\Gamma$, an increase to $J = \Gamma$ apparently leads back to Franck–Condon blocking. Here, $J = \Gamma$ approximately corresponds to the case of instantaneous IVR on the time scale of charge transmission, where all vibrational population

is in the ground state. Comparison with the $E_R = 0$ limit shows that rapid IVR even delays the appearance of the current but at the same time leads to a more rapid switch-on behavior. Interestingly, at large voltages, the current for strong IVR exceeds that of the weak IVR case. Analysis shows that this is due to a more efficient transfer from the state $|\chi_{0g0}\rangle$ as compared to the case of population distribution over several vibrational states (cf. Figure 3b). In contrast, optical switching is rather robust with respect to the increase of the decay rate r_{dec} . This is a consequence of the fact that, within the present model, $K_{\text{Neg}}^{(\text{dec})}$ merely maps the excited-state distribution onto the ground state according to $S_{\text{Ne},\text{Ng}}(\omega, \bar{\omega})$. Finally, we note that the IV curve for $J = \Gamma$ and $r_{\text{dec}} = 100\Gamma$ is almost identical to the $J = \Gamma$ and $r_{\text{dec}} = 0$ case, that is, IVR dominates the shape of the IV characteristics for the present model.

Summary. In conclusion, we have demonstrated photo-induced current switching of single-molecule charge transfer in the low-voltage regime where the Franck–Condon blockade due to strong nuclear rearrangement would otherwise be effective. The used generalized master equation approach provides the flexible frame not only for adoption to specific molecular systems but also for an extension to include, for instance, higher-order rates combining direct charging and discharge of the molecule with its optical excitation or accounting for coherent photon-assisted charge transmission.

Acknowledgment. We gratefully acknowledge financial support by the Deutsche Forschungsgemeinschaft through Sonderforschungsbereich 450 and stimulating discussions with E. G. Petrov (Kiev) and P. Hänggi (Augsburg).

References

- (1) Adams, D. M.; Brus, L.; Chidsey, C. E. D. *J. Phys. Chem. B* **2003**, *107*, 6668.
- (2) Cuniberti, G.; Fagas, G.; Richter, K., Eds., *Introducing Molecular Electronics*; Lecture Notes in Physics, Vol. 680; Springer: Heidelberg, 2005.
- (3) (a) Chen, Y. N.; Chuu, D. S.; Brandes, T. *Phys. Rev. Lett.* **2003**, *90*, 166802. (b) Cota, E.; Aguado, R.; Platero, G. *Phys. Rev. Lett.* **2005**, *94*, 107202.
- (4) (a) Zhitenev, N. B.; Meng, H.; Bao, Z. *Phys. Rev. Lett.* **2002**, *88*, 226801. (b) Seideman, T. *J. Phys.: Condens. Matter* **2003**, *15*, R521. (c) Qiu, X. H.; Nazin, G. V. W.; Ho, H. *Phys. Rev. Lett.* **2004**, *92*, 206102. (d) Benesch, C.; Cířzek, M.; Thoss, M.; Domcke, W. *Chem. Phys. Lett.* **2006**, *430*, 355. (e) Galperin, M.; Nitzan, A. *J. Phys.: Condens. Matter* **2007**, *19*, 103201.
- (5) Koch, J.; von Oppen, F. *Phys. Rev. Lett.* **2005**, *94*, 206804.
- (6) May, V.; Kühn, O. *Chem. Phys. Lett.* **2006**, *420*, 192.
- (7) (a) Dulić, D.; van der Molen, S. J.; Kudernac, T. *Phys. Rev. Lett.* **2003**, *91*, 207402. (b) Yasutomi, S.; Morita, T.; Imanishi, Y.; Kimur, S. *Science* **2004**, *304*, 1944. (c) Wu, S. W.; Ogawa, N.; Ho, W. *Science* **2006**, *312*, 1262. (d) Brixner, T.; de Abajo, F. J. G.; Schneider, J.; Spindler, C.; Pfeiffer, W. *Phys. Rev. B* **2006**, *73*, 125437. (e) Guhr, D. C.; Rettinger, D.; Boneberg, J.; Erbe, A.; Leiderer, P.; Scheer, E. *Phys. Rev. Lett.* **2007**, *99*, 086801.
- (8) Kohler, S.; Lehmann, J.; Hänggi, P. *Phys. Rep.* **2005**, *406*, 379.
- (9) (a) Kohler, S.; Hänggi, P. *Nat. Nanotechnol.* **2007**, *2*, 675. (b) Li, C. Q.; Schreiber, M.; Kleinekathöfer, U. *Europhys. Lett.* **2007**, *79*, 27006. (c) Franco, I.; Shapiro, M.; Brumer, P. *Phys. Rev. Lett.* **2007**, *99*, 126802.
- (10) Lehmann, J.; Kohler, S.; May, V.; Hänggi, P. *J. Chem. Phys.* **2004**, *121*, 2278.
- (11) (a) Boker, J.; Kirczenow, G. *Phys. Rev. B* **2002**, *66*, 245306. (b) Hettler, M. H.; Wenzel, W.; Wegewijs, M. R.; Schoeller, H. *Phys. Rev. Lett.* **2003**, *90*, 076805.
- (12) (a) Galperin, M.; Nitzan, A. *Phys. Rev. Lett.* **2005**, *95*, 206802. (b) Galperin, M.; Nitzan, A. *J. Chem. Phys.* **2006**, *124*, 234709.
- (13) Maddox, J. B.; Harbola, U.; Bazan, G. C.; Mukamel, S. *Chem. Phys. Lett.* **2007**, *450*, 144.
- (14) May V.; Kühn, O., *Phys. Rev. B* **2008**, in press.
- (15) May V.; Kühn, O. *Charge and Energy Transfer Dynamics in Molecular Systems*; Wiley-VCH: Weinheim, 2004.

NL073150H